Progress In Electromagnetics Research B, Vol. 29, 233–250, 2011

BANDWIDTH ENHANCEMENT OF CIRCULARLY POLARIZED SQUARE SLOT ANTENNA

R. Joseph and T. Fukusako

Kumamoto University
2-39-1 Kurokami, Kumamoto 860-8555, Japan

Abstract—Bandwidth enhancement technique of circularly polarized square slot antenna is presented in this paper. A square slot antenna with the components of L-probe separated could achieve an axial ratio (AR) bandwidth of 33.84%. Placing Stubs in the slot by studying the electric field behaviour could enhance the AR bandwidth by around 10%. Creating an L-shaped slot on the ground plane, where the electric field rotates in the desired clockwise direction, can further enhance the bandwidth by 7%. A < -10 dB S_{11} bandwidth of 46.15% and < 3 dB AR bandwidth of 50.35% could be achieved with the present design. Unidirectional patters are obtained by having a cavity at the wide slot of the antenna and shows a measured bandwidth of 41.79% in S_{11} and 44.97% in AR. Both antennas show a cross polarization discrimination of more than 15 dB on a wide azimuth range. The measured results well comply with the simulated results.

1. INTRODUCTION

Circularly polarized (CP) antennas are preferred over linearly polarized antennas because they do not require alignment of electric field vector between the transmitter and receiver locations. So, CP antennas have been extensively studied and are well suited for applications in satellites, RADARs, GPS and mobile terminals [1–4]. Printed slot antennas [5–8] with wide radiating slot provide bidirectional radiation, i.e., simultaneous RHCP and LHCP, and have been used in satellite digital radio systems [5] and for the reception of terrestrial signals and signals of geostationary satellites [6]. They also provide wider bandwidth without increasing the antenna size and thickness along

Received 4 March 2011, Accepted 30 March 2011, Scheduled 1 April 2011
Corresponding author: Ronald Joseph (ronald@st.cs.kumamoto-u.ac.jp).

with greater manufacturing tolerances [7]. Since the polarization sense changes from RHCP to LHCP and vice versa when reflected, an antenna which could receive both senses is significant, when the antenna needs to receive the reflected signal, if the direct signal is obstructed.

The planar circular slot antenna in [7] has achieved an impedance and CP bandwidth of 38% and 44% respectively but the antenna has a size of 100×100 mm. Truncating one of the corners of the antenna fed by L-shaped feed probe to enhance the bandwidth in [8] has claimed to have an overlapped bandwidth of 46.5%. But both these structures show high cross polarization except in the bore sight direction.

In the present paper, we propose bandwidth enhancement techniques using a square slot antenna for planar and cavity-backed structures. Rectangular aperture antenna is the common microwave antenna because the rectangular coordinate system is the most convenient system to express the field at the aperture. Also the cavity designed based on the rectangular waveguide principle provides wider bandwidth compared to circular cavity backed antenna since the frequencies of the dominant mode and the next higher order mode are wide apart [9]. A planar square slot antenna, could obtain a CP bandwidth of only 33.84%. The effect of placing stubs in the slot, which could control the undesired electric field rotations in the slot, is proposed to improve the AR bandwidth to 43.75%, approximately 10% more than the previous case. Having an additional L-shaped slot on the right side top corner of the ground plane could further improve the CP bandwidth by another 7%, to 50.35%. The proposed antenna has around 20% reduction in size compared to [7] and much wider bandwidth compared to the antennas in [7] and [8]. Also the antenna shows good cross polarization discrimination of more than 15 dB, not only in the bore sight direction but also on a wide azimuth range of more than 50°, for all the measured frequencies, to that proposed in [7, 8].

Since unidirectional patterns are required for applications in WLAN and pulse RADARs [10–13], a square cavity is made at the wide slot of the proposed planar antenna. An inverted microstrip-fed cavity backed antenna presented in [12], has a CP bandwidth of only 15%. The single element antenna presented in [13], claimed a CP bandwidth of 24%. A CP bandwidth of 44.97% is achieved with the proposed square cavity backed antenna. This bandwidth is much wider than the bandwidth of 36.13%, obtained by the circular cavity backed antenna in our previous paper [14] and [12, 13]. The simulated input and far field characteristics are compared with the experimental results and are in good agreement.

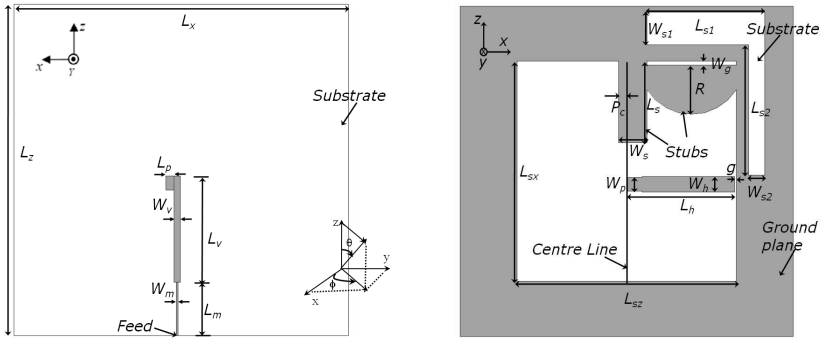

Figure 1. Antenna with stubs and additional L-slot. (a) Front View. (b) Back View.

2. PLANAR SQUARE SLOT ANTENNA

The structure of the antenna is shown in Figure 1. The antenna is designed at a centre frequency of 3 GHz and uses a 0.8 mm thick Arlon Diclad 522 substrate with a permittivity (ϵ_r) of 2.5 and a dielectric loss ($\tan\delta$) of 0.001. Arlon Diclad 522 is chosen as the substrate because it demonstrates good stability of dielectric constant across frequency. It also provides better dimensional stability and lower thermal expansion in all direction. At the same time, the substrate is very thin and suitable for low profile antenna structures. The substrate dimensions are $L_x = 82\,\text{mm}$ and $L_z = 81\,\text{mm}$, which are at $0.82\lambda_0$ and $0.81\lambda_0$ respectively, where λ_0 is the wavelength at the centre frequency of 3 GHz. The square slot has a dimension of $L_{sx} = L_{sz} = 54\,\text{mm}$ and is designed to be around $\lambda_0/2$ of the centre frequency. The L-probe is fed through a $118\,\Omega$ inductive microstrip feed line which has a width (W_m) of 0.4 mm and length (L_m) of 13.5 mm. This is to cancel off the capacitive impedance at the edge of the slot of the antenna and to match with the impedance of the $50\,\Omega$ feeding coaxial cable.

The vertical and horizontal components of the L-shaped probe respectively generate the E_θ and E_ϕ constituents of the CP. The vertical probe that succeeds the microstrip feed line, designed at around $\lambda_0/4$ of the centre frequency, is 26 mm long (L_v) and 1 mm wide (W_v). The phase condition of CP prominently depends on this parameter.

The horizontal and vertical components of the L-shaped probe are separated and placed on the front and backside of the substrate to enhance the capacitance in the antenna. By incorporating capacitance

in the antenna, the phase difference can be set to 90°, which yields to broadband CP. A 2-mm long patch (L_p) of 3.4-mm width is attached at the end of the vertical probe, also to enhance the capacitance. The horizontal component of the L-probe has a length (L_h) of 26.15 mm but has uneven widths. The region of the horizontal probe at the centre of the slot equals the width (W_p) of patch, L_p, placed at the front side of the substrate. The remaining portion of the horizontal probe has a width (W_h) of 3.8 mm. A 0.1 mm gap (g) is made between the horizontal probe and the ground plane, also to enhance the capacitance.

Different parametric studies are conducted on the antenna using Ansoft HFSS 10.1 simulation software, which utilizes 3D full wave finite element method (FEM).

The design of the antenna for the bandwidth enhancement of CP is carried out by studying the electric field vector behaviour in the slot. This is a provision equipped with the new versions of HFSS. The proposed CP antenna is designed to generate RHCP in the bore sight direction. So the antenna should show complete clockwise rotations in the entire slot. If there are counter clockwise rotations, it will lead to high cross polarization and deterioration of AR. Covering the region of counter clockwise rotations with metal is the normal way of solving this problem. But the antenna will have high cross polarization levels except in the bore sight direction. We propose here with placing stubs in the slot to eliminate counter clockwise rotations. The position and the size of the stubs should be optimized through parametric studies. A complete clockwise rotation in the slot with minimum number of stubs could lead to wideband CP with good cross polarization discrimination (XPD) on a wide azimuth range. Bandwidth could be further enhanced by selectively creating additional slot in the antenna. The electric field vector in the additional slot should also possess clockwise rotations so that wideband CP could be obtained.

The antenna is initially analysed with a square slot, without having any stubs in the slot and additional L-slot at the top right corner of the ground plane. The CP bandwidth was only 33.84% even after optimizing different parameters of the antenna. In order to enhance the bandwidth, the electric field vector behaviour in the slot of the antenna at the centre frequency, 3 GHz, for one complete cycle is studied and is shown in Figure 2. 0°, 120° and 240° represents the polarization phase of the electric field vector at the respective instances.

A complete clockwise rotation of the electric field vector in the entire slot is required to have broadband CP. But at the marked region in the slot, the electric field vector shows undesired counter clockwise rotations. Stubs are placed in the slot to eliminate these

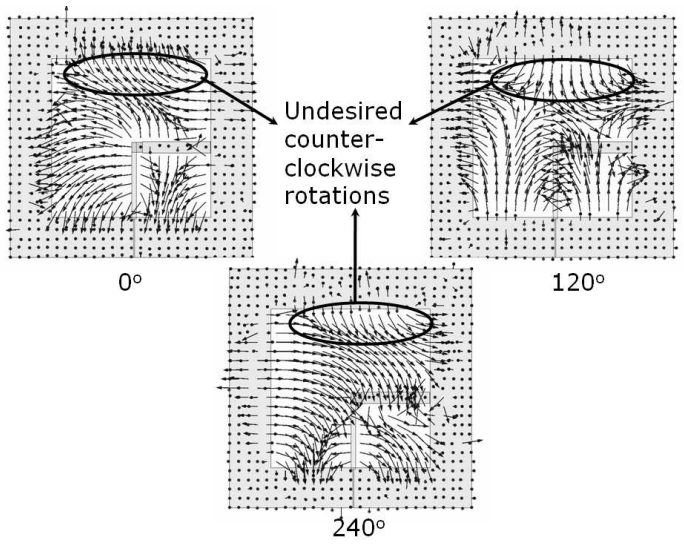

Figure 2. Electric field vector behaviour in the slot at 3 GHz.

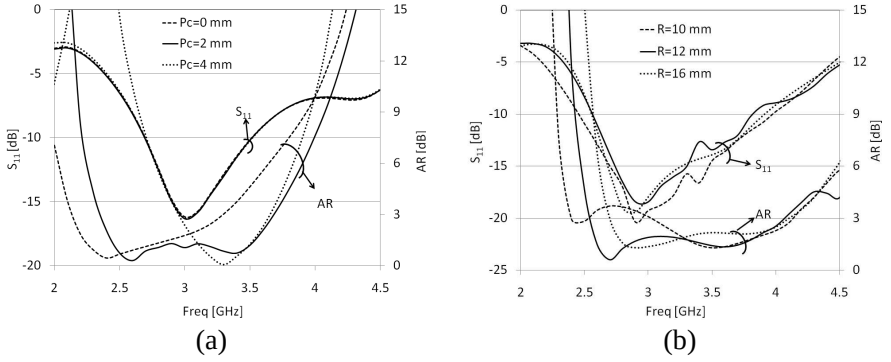

Figure 3. Effect of stubs' parameters on S_{11} and AR characteristics. (a) Effect of distance P_c. (b) Effect of radius R.

counter clockwise rotations. The shapes of the stubs are arbitrarily chosen but the size and position are optimized through parametric studies. A rectangular stub, offset from the centre, P_c, by 2 mm and a semicircular stub with a radius R of 12 mm could be placed in the slot to eliminate the counter clockwise rotations. Initially the antenna was analysed with only the rectangular stub of width $W_s = 7$ mm and length $L_s = 20$ mm. The position of this stub, P_c, considerably affects the AR characteristics. The effect of P_c on S_{11} and AR characteristics are shown in Figure 3(a).

The position of the rectangular stub does not affect the antenna's impedance characteristics. The resonance frequency and the bandwidth remain the same even for a variation of 4 mm from the centre. The antenna could attain broadband AR characteristics of 40.15% from 2.41 GHz to 3.62 GHz, when $P_c = 2$ mm. When P_c is at 0 mm, the counter clockwise rotation is divided in to the left and right sides of the stub. At 2 mm and 4 mm of P_c, the stub could confine the counter clockwise rotations to the right side top corner of the slot. But the area of counter clockwise rotation at 0 mm and 4 mm is larger than that at $P_c = 2$ mm.

Placing only the rectangular stub could not completely eliminate the counter clockwise rotations. In order to attain complete clockwise rotation in the slot, a semi-circular stub is placed in the slot in such a way that, it creates a 22-mm long rectangular slot of width $W_g = 1$ mm. The radius, R, of this stub and the gap W_g affect the antenna characteristics and are shown in Figure 3(b) and Figure 4 respectively.

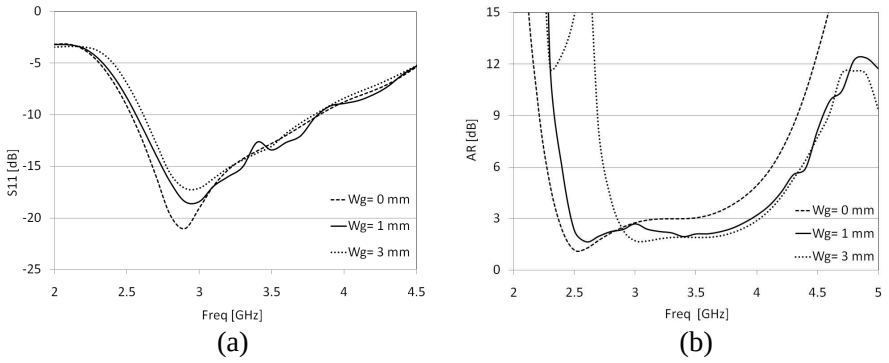

Figure 4. Effect of gap W_g. (a) S_{11} characteristics. (b) AR characteristics ($+y$ dir.).

The antenna shows slight variation in the impedance characteristics with the variation in R. The resonance frequency of the antenna almost remains unchanged for $R = 10$ mm to 16 mm. Placing of the stub in the slot is mainly used to broaden the AR band. A stub radius of 10 mm is not sufficient enough to cover up the area of counter clockwise rotation. When the radius is 16 mm, the stub disturbs the electric field in the region with clockwise rotation. This leads to counter clockwise rotation in the slot and narrows down the AR bandwidth.

The effect of the gap W_g, presented in Figure 4, shows that the resonance frequency and the S_{11} bandwidth remain almost unchanged

with variation in W_g but affects the AR characteristics. As W_g increases from 1 mm to 3 mm, E_ϕ becomes stronger than E_θ and the amplitude ratio between E_ϕ and E_θ becomes 6 dB at 2.7 GHz. A W_g of 1 mm provides wideband AR of 43.75% (2.5 GHz to 3.9 GHz) and S_{11} bandwidth of 41.8% (2.55 GHz to 3.9 GHz).

The antenna bandwidth can be further improved by creating an additional L-shaped slot on the top right corner of the ground plane. This should be done very carefully because counter clockwise rotations of electric field in this slot will lead to the deterioration of AR. Different parametric studies are conducted to optimize the position and the parameters of this slot.

The horizontal and vertical portions of the L-slot are made at a distance of 1.5 mm and 7 mm away from the edge. After optimizing the length L_{s1} and width W_{s1} of the horizontal part to 29 mm and 8 mm respectively, the parameters of the vertical portion of the L-slot are optimized. Keeping the width W_{s2} at 4 mm, the length L_{s2} of the slot is varied and the effect of which on S_{11} and AR characteristics is shown in Figure 5. This parameter considerably affects the antenna characteristics.

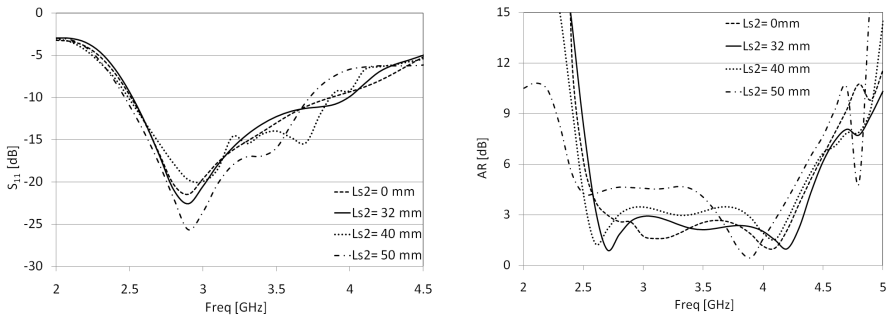

Figure 5. Effect of length L_{s2}. (a) S_{11} characteristics. (b) AR characteristics ($+y$ dir.).

The S_{11} characteristics show wider bandwidth compared to the design without the additional L-slot. The bandwidth is slightly narrowed when the length, L_{s2}, is increased from 32 mm to 50 mm, since the impedance becomes more inductive at higher frequencies. As far as AR characteristics are concerned, there need be clockwise rotations of the electric field vector even in the created slot. But as the length increases from 32 mm, the lower regions of the slot turned out to have counter clockwise rotations. This deteriorates the AR bandwidth. A length L_{s2} of 32 mm leads to an AR bandwidth of

50.35% from 2.6 GHz to 4.35 GHz and S_{11} bandwidth of 46.15% from 2.5 GHz to 4 GHz.

The electric field vector behaviour in the slot of the antenna at the centre frequency (3 GHz) is shown in Figure 6. It could be observed that in the wide slot as well as in the *L*-slot, the electric field rotates in the clockwise direction and because of which broadband CP is achieved.

In an attempt to further improve the bandwidth, we studied the electric field vector behaviour in the slot of the antenna at 4.2 GHz and is shown in Figure 7. The antenna shows complex electric field vector rotations, a combination of clock wise and counter clockwise rotations in the slot. But the antenna has good AR at 4.2 GHz. This is because of

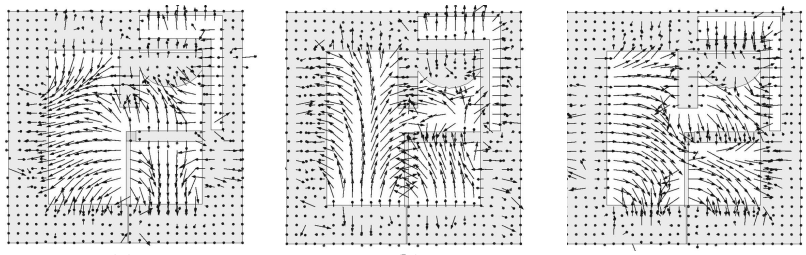

Figure 6. Electric field vector behaviour in the slot at 3 GHz. (a) 0°. (b) 120°. (c) 240°.

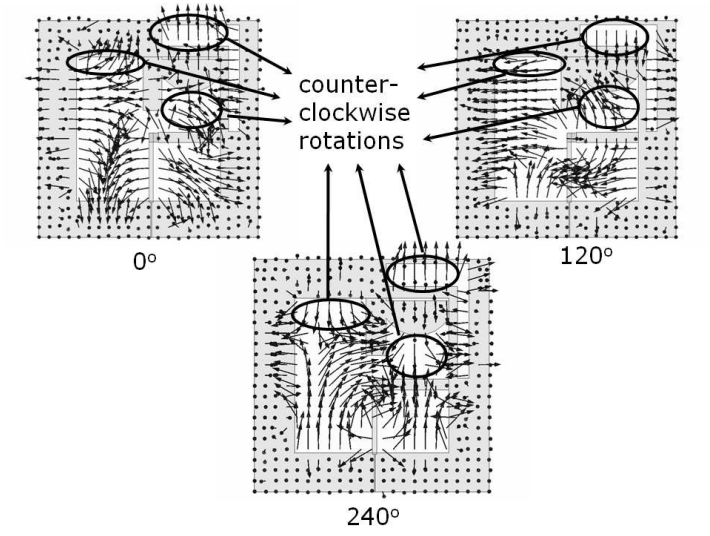

Figure 7. Electric field vector behaviour in the slot at 4.2 GHz.

the fact that AR is determined by the synthesized result of amplitude and phase difference of the two orthogonal electric field components E_ϕ and E_θ, which are nearly 0 dB and 90° at this frequency. Covering the regions with the stubs to eliminate counter clockwise rotations make the antenna structure more complicated and need tuning of basic antenna parameters. So the antenna was not modified further.

For comparison, the S_{11}, AR (at $\theta = \phi = 90°$, i.e., in the $+y$ direction) and phase difference characteristics of the antennas are presented in Figure 8. The antenna's are named as *ant 1* (antenna without stubs and L-slot), *ant 2* (antenna with stubs without L-slot) and *ant 3* (antenna with stubs and L-slot) respectively.

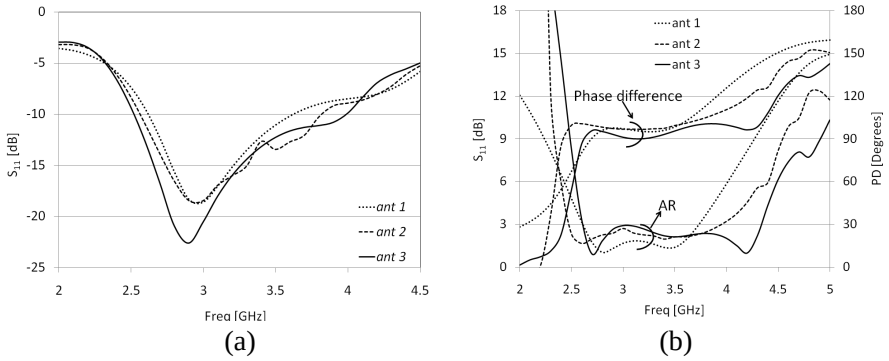

Figure 8. Comparison of antennas. (a) S_{11} characteristics. (b) AR and phase difference characteristics.

The bandwidth is enhanced in S_{11} characteristics from *ant 1* to *ant 3* because the antenna becomes more capacitive with the addition of stubs and L-slot. The resonance frequency of the antenna remains unchanged but the < -10 dB S_{11} bandwidth is improved from 37.5% to 41.8% to 46.15% from *ant 1* to *ant 2* to *ant 3*. The addition of stubs and L-slot mainly controls the phase difference between E_ϕ and E_θ and can be set to nearly 90° (Figure 8(b)) on a wide band with the implementation of stubs and L-slot. So the AR bandwidth can be enhanced in *ant 3*, to 50.35% from 33.84% of *ant 1*.

2.1. Experimental Results

The antenna with stubs and L-slot (*ant 3*) is fabricated on an Arlon Diclad 522 substrate with thickness of 0.8 mm. The simulated and measured S_{11} characteristics of the antenna are shown in Figure 9(a). The antenna resonates at around 3 GHz and the measured characteristics are well matched with the simulated results. A $<$

−10 dB bandwidth of 46.15% from 2.5 GHz to 4 GHz is obtained in simulation as well as in measurement. The simulated AR characteristics in Figure 9(b) show broadband characteristics of 50.35% from 2.6 GHz to 4.35 GHz. The measured characteristics are well

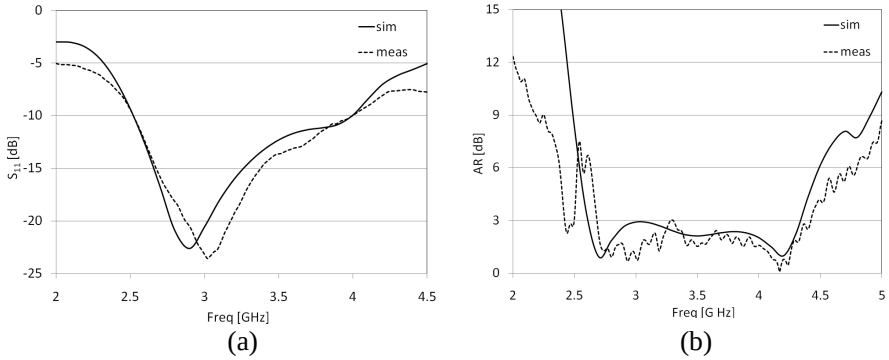

Figure 9. Characteristics of the antenna. (a) S_{11} characteristics. (b) AR characteristics ($+y$ dir.).

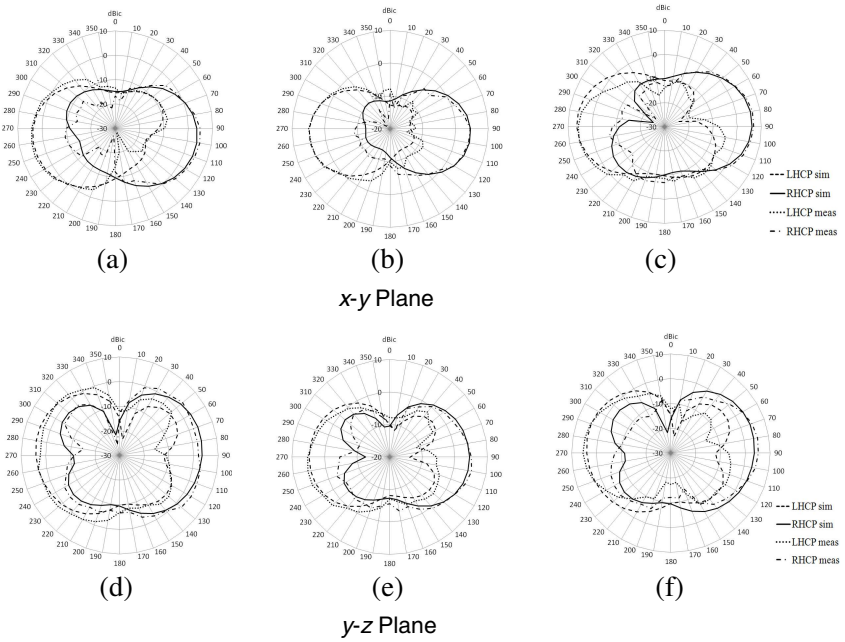

Figure 10. Radiation pattern. (a) 3 GHz. (b) 3.5 GHz. (c) 4 GHz. (d) 3 GHz. (e) 3.5 GHz. (f) 4 GHz.

complied with the simulated results and show a bandwidth of 50.14% from 2.66 GHz to 4.44 GHz.

The far field radiation pattern characteristics of the antenna in x-y and y-z plane at 3 GHz, 3.5 GHz and 4 GHz are simulated and measured. The results are shown in Figure 10. The antenna shows bidirectional radiation patterns since it is a slot antenna. The radiation pattern in the x-y plane shows a XPD of more than 15 dB on a wide azimuth range from 80° to 130°, 70° to 130° and 50° to 100° at 3 GHz, 3.5 GHz and 4 GHz. Also a front to back (FB) ratio of around 18 dB is obtained in all the three cases. The simulated and measured radiation pattern characteristics in the y-z plane are also in good agreement. A XPD of 15 dB from 70° to 100° at 3 GHz and 3.5 GHz and 12 dB from 80° to 110° at 4 GHz are obtained. The FB ratio is more than 15 dB in all the cases.

The simulated and measured gain characteristics of the antenna in the $+y$ direction ($\theta = \phi = 90°$) are shown in Figure 11. The two characteristics agree each other very well. A maximum gain of 5.45 dBic is obtained in simulation as well as in measurement.

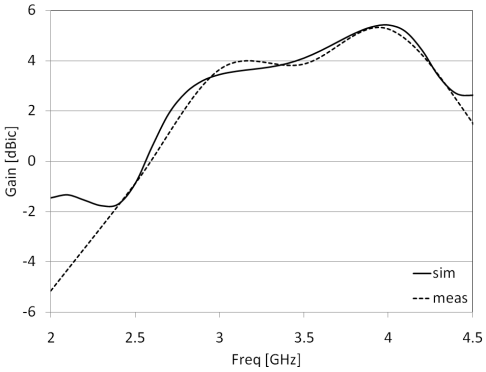

Figure 11. Gain characteristics ($+y$ dir.).

The proposed planar CP broadband antenna is a promising candidate for chipless RFID [15] and cognitive radio systems [16].

3. CAVITY-BACKED ANTENNA

As mentioned in Section 1, unidirectional radiation patterns are required for applications in pulse RADARs and telecommunications because of the security and efficiency along with wideband operation. So a reflector or a cavity can be installed to a slot antenna to obtain unidirectional patterns. Installing a cavity or a reflector will lead to the

deterioration of the antenna characteristics. So some of the antenna parameters are to be optimized to achieve broadband characteristics.

Initially the cavity was placed at the edge of the antenna, but unable to generate wideband CP. So, the cavity is designed to be at the wide slot instead of being at the edge of the antenna. The L-slot is removed from the structure because it radiates bidirectional radiation since outside the cavity. The structure of the antenna is shown in the Figure 12.

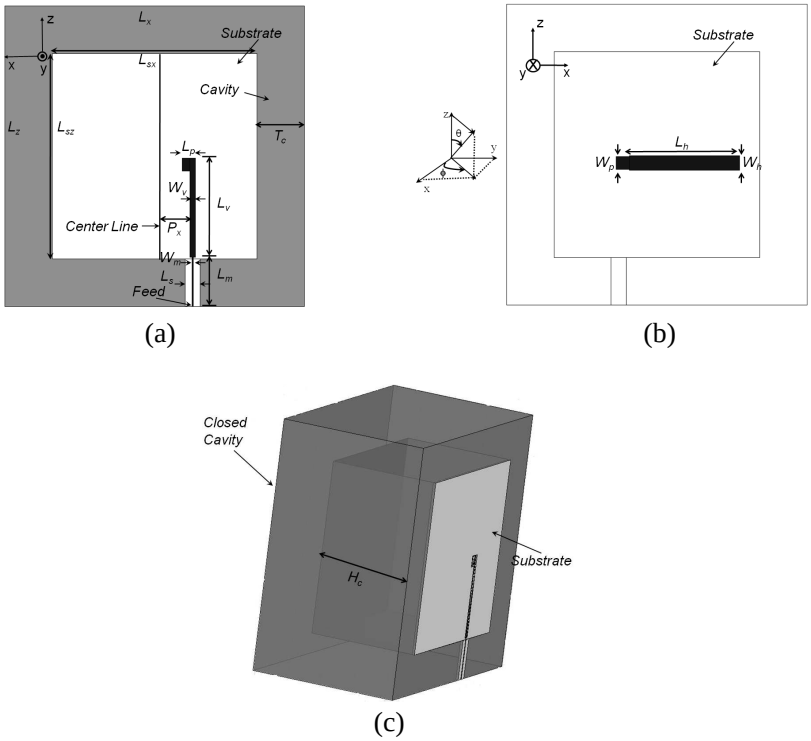

Figure 12. Cavity backed antenna. (a) Front view. (b) Transparent back view. (c) 3 dimensional view.

The cavity is designed based on the principle of rectangular waveguide, as explained in [17]. The cut-off frequencies of different propagating modes through the waveguide are determined by the formula

$$f_{c_{(mn)}} = \frac{1}{2\pi\sqrt{\mu_o \epsilon_o}} \sqrt{\left(\frac{m\pi}{a}\right)^2 + \left(\frac{n\pi}{b}\right)^2}$$

where m and n represent the mode of propagation and indicates the

number of variations of the field in the x and y directions, a and b are the length and breadth of the waveguide, ϵ_o and μ_o are the permittivity and permeability in the free space respectively.

The dominant mode, TE_{10}/TE_{01}, and the next higher order mode, TE_{11}/TM_{11}, have their cut-off frequencies at 2.77 GHz and 6.25 GHz respectively, when $a = b = 54$ mm. The centre frequency of operation is fixed at 3.5 GHz, higher than the dominant mode frequency. This frequency is selected so that the antenna can be used, for example, in 3.5 GHz WiMAX [18], WLAN [19] and pulse RADARs. The height of the cavity (H_c) is fixed to be at 35 mm, which is at $\lambda_g/4$, where λ_g is the guided wavelength and designed by the formula

$$\lambda_g = \frac{\lambda}{\sqrt{1 - \left(\frac{f_c}{f}\right)^2}}$$

where f and λ are the frequency and corresponding wavelength in free space and f_c is the frequency at the dominant mode.

The initial analyses of the antenna were carried out with a cavity wall thickness of 1.5 mm and without having any stubs in the slot. The observed electric field vector behaviour at polarization phases of 0°, 120° and 240° is shown in Figure 13. The electric field rotates completely in the clockwise direction and does not require any stubs in the slot. This is because of the radiated LHCP signal towards the closed cavity changes its polarization sense to RHCP when reflected. This signal incidents on the antenna and leads to complete clockwise rotation in the slot.

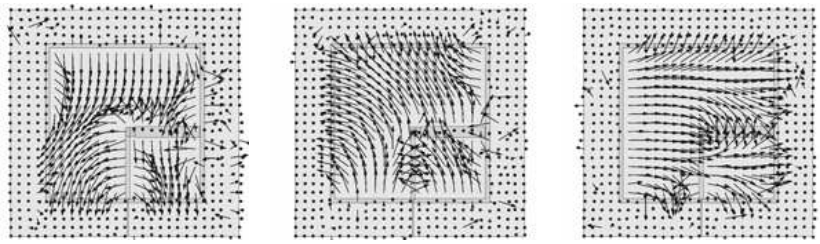

Figure 13. Electric field vector behaviour at 3.5 GHz. (a) 0°. (b) 120°. (c) 240°.

In order to obtain wideband CP, the position of the feed line (P_x) along with the vertical and horizontal probes are shifted from the centre of the cavity, in the negative x-axis, and the effect of which is shown in Figure 14. The antenna could obtain wideband S_{11} characteristics

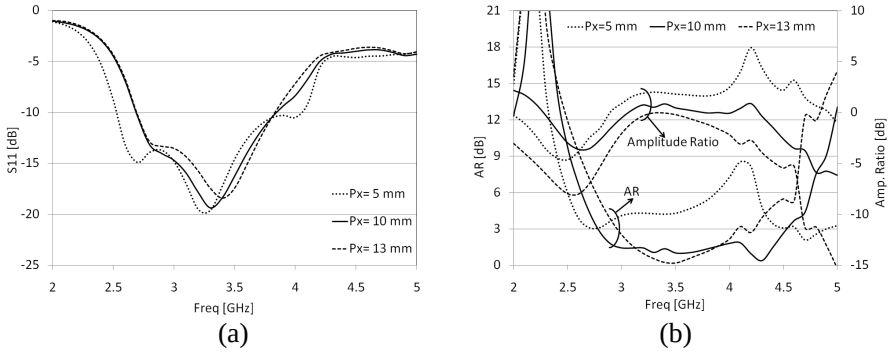

Figure 14. Effect of position of the feed from the centre (P_x). (a) S_{11} characteristics. (b) AR and amplitude ratio characteristics.

even when the probe is at the centre and are not much affected by the shift. When the feed probe is at the centre, E_θ is stronger than E_ϕ and the amplitude ratio is around 3.5 dB at 3.5 GHz. There exists strong electric field between the gap of horizontal probe and the cavity, which is a responsible component for the generation of the E_ϕ constituent of the CP. Shifting the probe in the negative x-axis could make E_ϕ stronger, as the gap between the horizontal probe and the cavity is increased. A shift by 10 mm makes the amplitude of the two orthogonal components nearly equal (Figure 14(b)) and the phase difference to be around 90° to generate broadband CP. An AR bandwidth of 44.89% (2.85 GHz–4.5 GHz) is achieved but the S_{11} bandwidth is only 33.8% (2.7 GHz–3.8 GHz).

For improving the S_{11} bandwidth, the length of the microstrip feed line, L_m, is shortened by 0.5 mm, i.e, to 13 mm from 13.5 mm. Also the width of the vertical probe W_v is increased from 1 mm to 1.5 mm. The antenna could attain an S_{11} bandwidth of 41.79% (2.65 GHz–4.05 GHz) and AR bandwidth of 44.97% (2.69 GHz–4.25 GHz).

Also it could be observed from Figure 13 that the electric field is confined in the cavity. So the substrate and ground plane outside the slot, except the region below the micostrip feed line, are removed and noticed that it does not affect the antenna characteristics. The substrate and the ground plane beneath the feeding microstrip line has a width of L_s. This width, L_s, can be as small as 4 mm, but smaller widths deteriorates the characteristics since the microstrip feed line will be at close proximity with the cavity wall.

The thickness of the cavity, T_c, also does not affect the antenna characteristics. A thicker cavity of 12.5 mm is preferred because it could be neatly fabricated and will not be easily mangled.

3.1. Experimental Results

The above antenna is fabricated with a cavity made of aluminium and the simulated and experimental results of S_{11} and AR are presented in Figure 15.

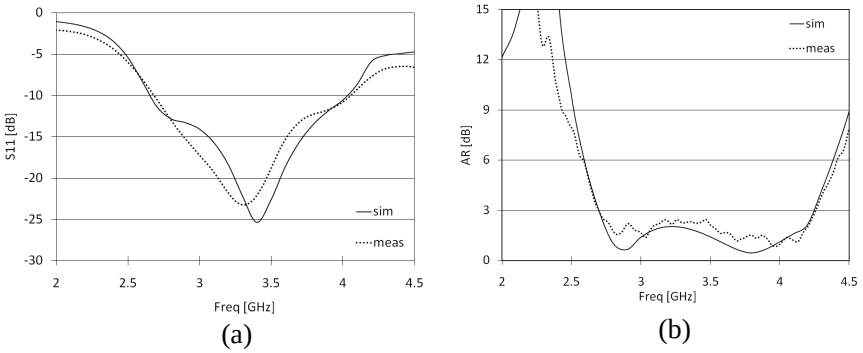

Figure 15. Characteristics of the antenna. (a) S_{11} characteristics. (b) AR characteristics ($+y$ dir.).

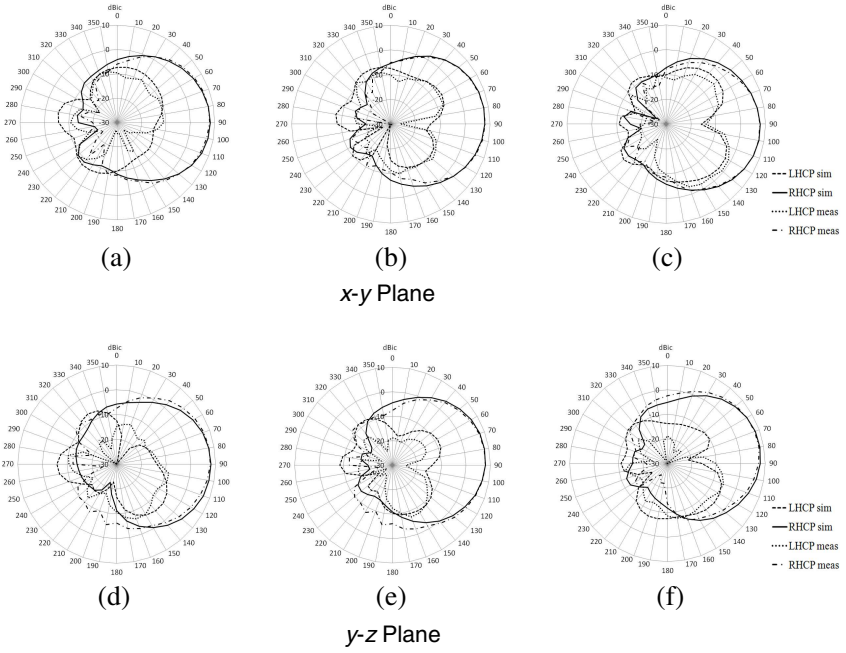

Figure 16. Radiation pattern. (a) 3 GHz. (b) 3.5 GHz. (c) 4 GHz. (d) 3 GHz. (e) 3.5 GHz. (f) 4 GHz.

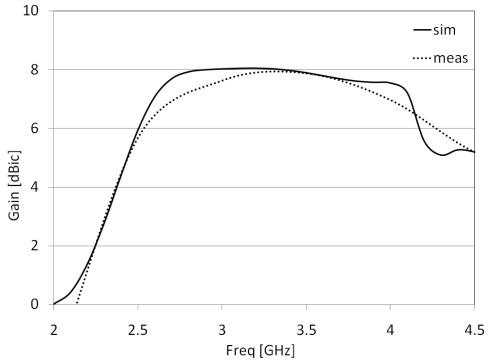

Figure 17. Gain characteristics ($+y$ dir.).

The measured and simulated S_{11} characteristics are well matched and shows a < -10 dB bandwidth of 41.79% (2.65 GHz–4.05 GHz). An AR bandwidth of 44.97% (2.69 GHz–4.25 GHz) at < 3 dB, both in simulation and measurement is also obtained.

The radiation pattern characteristics of the cavity backed antenna is shown in Figure 16. The antenna shows very good XPD of more than 15 dB from 50° to 130°, 60° to 120° and 70° to 100° at 3 GHz, 3.5 GHz and 4 GHz respectively in the x-y plane. A FB ratio of around 25 dB could be achieved in all the cases. A XPD of more than 15 dB is also obtained in y-z plane from 40° to 110°, 40° to 120° and 40° to 100° at 3 GHz, 3.5 GHz and 4 GHz respectively. Even the FB ratio is around 25 dB at all the three instances.

The gain characteristics presented in Figure 17 show almost constant gain in the operating band. The simulated and measured characteristics are in good agreement and achieves a maximum gain of 8 dBic.

4. CONCLUSIONS

A novel technique of bandwidth enhancement for planar circularly polarized slot antenna is presented in this paper. Changing the slot aperture by placing appropriate stubs in the slot by observing the electric field behaviour is proposed to eliminate the undesired electric field rotations and enhance the AR bandwidth by around 10%. In order to further improve the bandwidth, creating an additional L-slot on the ground plane of the antenna is also presented. These techniques to enhance the bandwidth are effective and well suited for planar slot antenna structures. In cavity backed antennas, the cavity itself

takes care of the counter clockwise rotations develop in the slot and invalidate the need of stubs. The proposed planar antenna could attain a CP bandwidth of 50.14% in measurement which is approximately 6% more than the bandwidth obtained in [14]. The measured S_{11} and CP bandwidth of the circular cavity backed antenna in [14] were 37.16% and 36.3%. These bandwidths could be improved to 41.79% and 44.97% respectively with the present square cavity backed antenna. A cross polarization discrimination of more than 15 dB on a wide azimuth range is obtained both in planar and cavity backed structures with the present design, along with a maximum gain of 5.45 dBic and 8 dBic, which are approximately same as in [14].

REFERENCES

1. Chen, H. M., Y. K. Wang, Y. F. Lin, C. Y. Lin, and S. C. Pan, "Microstrip FED circularly polarized square ring patch antenna for GPS application," *IEEE Trans. Anten. Propag.*, Vol. 57, No. 4, 1264–1267, Apr. 2009.
2. Liu, J.-C., B.-H. Zeng, C.-Y. Liu, H.-C. Wu, and H.-C. Chang, "A dual-mode aperture-coupled stack antenna for WLAN dual-band and circular polarization applications," *Progress In Electromagnetics Research C*, Vol. 17, 193–202, 2010.
3. Yang, S. S., K.-F. Lee, A. A. Kishk, and K.-M. Luk, "Design and study of wideband single feed circularly polarized microstrip antennas," *Progress In Electromagnetics Research*, Vol. 80, 45–61, 2008.
4. Fukusako, T., K. Okuhata, K. Yanagawa, and N. Mita, "Generation of circular polarization using rectangular waveguide with *L*-type probe," *IEICE Trans. Commun.*, Vol. 86, 7, Jul. 2003.
5. Saala, G., J. Hopf, and S. Lindenmeier, "Small satellite car antenna for simultaneous reception of LHCP and RHCP signals," *Third European Conf. on Anten. Propag.*, 2698–2700, Mar. 2009.
6. Saala, G., D. Muller, J. Hopf, and S. Lindenmeier, "Antenna with optimized pattern for simultaneous reception of terrestrial signals and signals of geostationary satellites," *Advances in Radio Science*, Vol. 8, 37–42, 2010.
7. Tseng, L. Y. and T. Y. Han, "Microstrip fed circular slot antenna for circular polarization," *Microw. Opt. Technol. Lett.*, Vol. 50, No. 4, 1056–1058, Apr. 2008.
8. Yang, S. S., A. A. Kishk, and F. S. Lee, "Wideband circularly polarized antenna with *L*-shaped slot," *IEEE Trans. Anten. and Propag.*, Vol. 56, No. 6, 1780–1783, 2008.

9. Balanis, C. A., *Antenna Theory Analysis and Design*, John Wiley and Sons, Inc., 1997.
10. Qu, S. W., C. H. Chan, and Q. Xue, "Ultrawideband composite cavity backed folded sectoral bowtie antenna with stable pattern and high gain," *IEEE Trans. Antennas Propag.*, Vol. 57, No. 8, 2478–2483, Aug. 2009.
11. Ghosh, B., S. N. Sinha, and M. V. Kartikeyan, "Radiation from cavity-backed fractal aperture antennas," *Progress In Electromagnetics Research C*, Vol. 11, 155–170, 2009.
12. Li, Q. and Z. Shen, "An inverted microstrip fed cavity backed slot antenna for circular polarization," *IEEE Antennas and Wireless Propag. Lett.*, Vol. 1, 190–192, 2002.
13. Hung, K. F. and Y. C. Lin, "Novel broadband circularly polarized cavity backed aperture antenna with travelling wave excitation," *IEEE Trans. Anten. Propag.*, Vol. 58, No. 1, 155–170, 2009.
14. Joseph, R., S. Nakao, and T. Fukusako, "Circular slot antennas using *L*-shaped probe for broadband circular polarization," *Progress In Electromagnetics Research C*, Vol. 18, 153–168, 2011.
15. Preradovic, S., I. Balbin, N. C. Karmakar, and G. Swiegers, "A novel chipless RFID system based on planar multiresonators for barcode replacement," *IEEE International Conference on RFID*, 289–296, Apr. 2008.
16. Wu, T., R. L. Li, S. Y. Eom, S. S. Myoung, K. Lim, J. Laskar, S. I. Jeon, M. M. Tentzeris, and W. F. Richards, "Switchable quad-band antennas for cognitive radio base station applications," *IEEE Trans. on Anten. Propag.*, Vol. 58, No. 5, 1468–1476, May 2010.
17. Pozar, D. M., *Microrwave Engineering*, John Wiley and Sons, Inc., 2005.
18. Masa-Campos, J. L. and F. Gonzalez-Fernandez, "Dual linear/circular polarized planar antenna with low profile double-layer polarizer of 45° tilted metallic strips for WiMAX applications," *Progress In Electromagnetics Research*, Vol. 98, 221–231, 2009.
19. Prakash, D. and R. Khanna, "Design and development of CPW-FED microstrip antenna for WLAN/WiMAX applications," *Progress In Electromagnetics Research C*, Vol. 17, 17–27, 2010.